

## **Valid simulation of the composite behavior of steel bridges**

Vahid Broujerdian<sup>1)</sup>, \*Abbas Ghadami<sup>2)</sup>, Ghazaleh Pourmoosavi<sup>3)</sup> and  
Peyman Mahyar<sup>4)</sup>

<sup>1), 2), 4)</sup> *Department of Civil Engineering, Iran University of Science and Technology,  
Tehran, Iran*

<sup>3)</sup> *Department of Civil Engineering, Tabriz Branch, Islamic Azad University, Tabriz, Iran*  
<sup>2)</sup> [Ghadami@civileng.iust.ac.ir](mailto:Ghadami@civileng.iust.ac.ir)

### **ABSTRACT**

This paper presents a reliable finite element modeling technique for composite steel I-girder bridges. For this purpose, the modeling of bridge components is discussed separately and a useful technique for simulating the interaction of concrete slab and steel girder is introduced. The numerical simulations were performed using the general-purpose finite element software package ABAQUS and the results were corroborated with the available experimental results. It showed that, the stress field in girder section and the crack propagation pattern in concrete slab can be accurately estimated using the proposed method. It is also shown that this technique can be used for S4R shell and C3D8R solid elements in simulating concrete slab. Another advantage of the presented method is to decrease the time needed for simulation comparing to the current methods.

**Keywords:** Finite element method; Composite action; Bridge; Concrete damage plasticity

## **1. INTRODUCTION**

### *1.1. Background*

In horizontally curved steel I-girder bridges, the torsional moment resulting from the curvature causes warping across the sections of girders, which results in non-uniform stress distribution in the flanges of the girders. To predict such a complex behavior, numerical simulations are frequently used which most of them are based on finite element (FE) method. The simulation must include the exact behavior of structural members such as concrete slab, steel girders, and cross-frames, which requires the selection of appropriate elements in finite element software and considering interaction between members.

---

<sup>1)</sup> Assistant Professor

<sup>2), 3), 4)</sup> Ph.D Student

In ABAQUS software (Hibbitt, Karlsson et al. 2012), there is a variety of elements to model different components of structures. If one dimension (thickness) of a component is significantly smaller than the two other dimensions, a shell element can be used to model its behavior. According to their behavior, shell elements, in ABAQUS/Standard, are categorized in three groups of: (1) general-purpose elements, (2) thin shell elements, and (3) thick shell elements. Table 1 shows such different types of shell elements. The general-purpose shell elements consider finite membrane strain and large rotations. These elements include the effects of transverse shear deformation and thickness change. However, the thin and thick shell elements are based on small strain formulation and the thickness of element is assumed to remain constant during the analysis. Furthermore, thick shell elements take into account the effect of transverse shear flexibility. However, thin shell elements ignore this effect and are based on the Kirchhoff constraint, which assumes that the shell normal remains orthogonal to the shell reference surface (Hibbitt, Karlsson et al. 2012).

Table 1 Types of shell elements in ABAQUS/Standard

General-purpose	Thin	Thick
S4,S4R,S3/S3R,SAX1,SAX2 ,SAX2T,SC6R,SC8R	STRI3,STRI65,S4R5 ,S8R5,S9R5,SAXA	S8R,S8RT

### 1.2. Literature review

In order to model composite deck systems, different techniques have been presented up to now. In some numerical simulations, shell elements of concrete slab and beam elements of girder were used with some amount of eccentricity (Chan and Chan 1999, Chen 1999, Barr, Eberhard et al. 2001, Shahawy and Huang 2001). In some other methods, concrete slab and girder web were modeled using shell elements, and girder flange was modeled using beam elements (Brockenbrough 1986, Tabsh and Tabatabai 2001). There are some other methods using shell elements to model the concrete slab and girders (Chung and Sotelino 2006) or using first order brick elements for concrete slab and shell elements for girders (Mabsout, Tarhini et al. 1997). An overview of the researches conducted to simulate the composite steel I-girder decks, are summarized in Tables 2-3 in terms of the elements used.

Table 2 The elements used in finite element modeling of steel girder in composite decks in recent studies

Refer Component	(Sharafbani and Linzell 2014)	(Davidson, Keller et al. 1996)	(Ashour 2010)	(Ozgur 2007)	(Hartmann 2005)	(Sanchez 2011)	(Maneetes 2001)	(Jung 2006)	(Cullen 2007)	(Hassel 2011)
Girder flange	S4R	Beam	B31	B31	S4R	B31	B31 S4R	B31	S4R	C3D8 R
Girder web	S4R	Shell	S4R	S4R	S4R	S4R	S4R	S4R	S4R	C3D8 R

Table 3 The elements used in finite element modeling of concrete slab in composite decks in recent studies

Refer Component	(Hassel 2011)	(Thevendran, Chen et al. 1999)	(Biggs, Barton et al. 2000)	(Baskar, Shanmugam et al. 2002)	(Barth and Wu 2006)	(Shapiro 2007)	(Lin, Fafard et al. 1991)
Concrete slab	Shell	Shell	Shell	Solid	Shell	Solid	Shell
Shear stud	MPC	MPC	MPC	MPC	MPC	Tie	Bar Element

An assessment of modeling strategies for composite curved steel I-girder bridges has been reported in reference (Chang and White 2008). It should be mentioned that, in reference (Chang and White 2008), concrete-steel interaction has been modeled with rigid beam elements or Multi-Point Constraints (MPCs).

## 2. AIMS AND SCOPES

Using appropriate elements for steel and concrete parts of composite decks and accurate modeling of the interaction between them is important, yet, very time-consuming tasks. Unfortunately, there is not a comprehensive guide in this regard. However, it is obvious that the improper modeling leads to inaccurate estimation of the bridge behavior, also, wrong determination of the stress and crack pattern distribution in the concrete slab deck. Behavior of composite bridges mainly depends on the force transmission mechanism between concrete slab and steel girder (Si Larbi, Ferrier et al. 2009, He, Liu et al. 2010). MPC constraints give acceptable results in this respect. However, using this method requires much accurate work on the node to node restraining elements of the concrete slab and the steel flange girder. Therefore, in this study, first, the modeling of the bridge components including steel girders, cross-frames, and concrete slab in ABAQUS software is discussed. This is followed by a discussion of a rapid and reliable method to model the composite behavior of the bridge. In order to evaluate the proposed method, results are compared to the other numerical and experimental researches.

### 3. NUMERICAL MODELING

#### 3.1. Constitutive modeling of concrete in ABAQUS

In order to model concrete behavior, the ABAQUS software has three different constitutive models. All models have been designed to have capability to model both reinforced and pure concrete. According to reference (Jung 2006), FE modeling of the concrete behavior has been widely prescribed by concrete damage plasticity (CDP) model. Therefore, in this paper, concrete behavior is simulated using CDP model which is proposed by Lubliner et al. (1989) and Lee & Fenves (1998) (Hibbitt, Karlsson et al. 2012). In this model, two main failure mechanisms in concrete are considered: tensional cracking and compressional crushing. Failure rate is evaluated by two variables of  $\tilde{\epsilon}_t^{pl}$  and  $\tilde{\epsilon}_c^{pl}$  which are related to the tensional and compressional failure mechanisms, respectively. These two variables are the equivalent tension and compression plastic strains, respectively.

##### 3.1.1. Tensile behavior

Tensional post-peak behavior is modeled with tensional hardening, which it makes possible defining the tensional softening behavior for cracked concrete. This behavior, also, makes it possible to consider concrete-rebar interaction in a simple way. Tensile hardening in the CDP model can be defined by post-peak stress-strain or crack energy method, which is also called GFI method. According to Fig. 1(a), post-peak stress is a function of cracking strain ( $\tilde{\epsilon}_t^{cr}$ ). The cracking strain is the difference between total strain and corresponding elastic strain of undamaged material, which is defined as:

$$e_t^{cr} = e_t - s_t / E_0 \quad (1)$$

As also, shown in Fig. 1(a), tensile plastic strain is calculated as:

$$e_t^{pl} = e_t^{cr} - \frac{d_t}{(1-d_t)} \frac{s_t}{E_0} \quad (2)$$

Where  $d_t$  is the tensile damage parameter. It must be noted that the functions of  $\sigma_t - \tilde{\epsilon}_t^{cr}$  and  $d_t - \tilde{\epsilon}_t^{cr}$  are calculated using experimental loading and unloading data, respectively, and fed into ABAQUS. A crack is assumed to initiate at a point, when the maximum principal plastic strain is positive at the point. The direction of the crack is considered normal to the maximum principal plastic strain (Hibbitt, Karlsson et al. 2012).

##### 3.1.2. Compressive behavior

Compressive stress-strain behavior of unreinforced concrete can be defined out of elastic range. Compressive behavior data can be defined as a function of inelastic strains ( $\tilde{\epsilon}_c^{pl}$ ) and, if desired, as a function of strain rate, temperature and other parameters. As shown in Fig. 1(b), the inelastic compressive strain is the difference between total strain and corresponding elastic strain of undamaged material, which is defined as:

$$\tilde{\epsilon}_c^{pl} = e_c - s_c / E_0 \quad (3)$$

As also shown in Fig. 1(b), compressive plastic strain is calculated as:

$$e_c^{\sim pl} = e_c^{\sim in} - \frac{d_c}{(1-d_c)} \frac{S_c}{E_0} \quad (4)$$

Where,  $d_c$  is the compressive damage parameter.

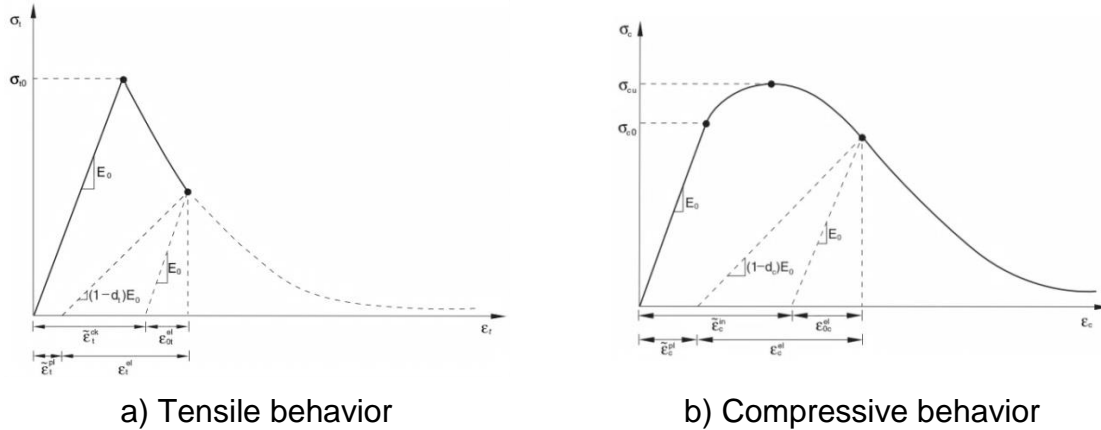


Fig. 1 Uniaxial stress-strain curve of concrete (Hibbitt, Karlsson et al. 2012)

### 3.2. Geometrical modeling of concrete slab, steel girders, and cross-frames

According to the prevalent method, as it can be seen in Table 3, shell element is used to model the concrete slab. In this type of elements, S4R takes into account the thickness shear deformation and large strain formulation. The behavior of this element, for thin and thick plates, is consistent with the classical plate theory and Mindlin-Reissner plate theory, respectively (Hibbitt, Karlsson et al. 2012). Therefore, S4R element is used for modeling concrete slab, in this study. According to reference (Jung 2006), the number of integration points is considered 9 through the thickness of the concrete slab. In ABAQUS, reinforcement in concrete structures is typically provided by means of rebars, which are one-dimensional rods that can be defined explicitly or embedded in oriented surfaces. Using this modeling method, concrete behavior is assumed independent from rebar behavior. Effects associated with the rebar/concrete interface, such as bond slip and dowel action, are modeled approximately by introducing some “tension stiffening” into the concrete modeling to simulate load transfer across cracks through the rebar. It must be noted that, the characteristics of the reinforcement materials are defined by elastic-perfectly plastic behavior (Jung 2006, Hibbitt, Karlsson et al. 2012). According to ABAQUS Manual, the preferred method for defining rebar in shell and membrane elements is defining layers of reinforcement as part of the element section definition.

Considering the results of the previous researches, listed in Table 2, due to the low thickness of the girder components in comparison with the other two dimensions, S4R element is used to simulate the girders.

To select an efficient element for cross-frames, two curved bridges were simulated by B31 and S4R elements, considering appropriate boundary conditions (Fig. 2). The overall behavior of these two models such as deck deflection, lateral displacement, etc. was very close. Thus, B31 element was selected in this study, because of its simplicity.

### 3.3. Simulating concrete-steel interaction using proposed method

In this study, concrete-steel interaction is considered as full composite action. In other words, it is assumed that, there is no relative sliding between concrete and steel. Instead of the conventional connecting technique of concrete and steel, that is MPC technique, Tie constraint is used in this study as shown in Fig. 3. In other words, using node to surface method, the connecting line of bottom surface of the concrete slab is tied to the compressive flange surface.

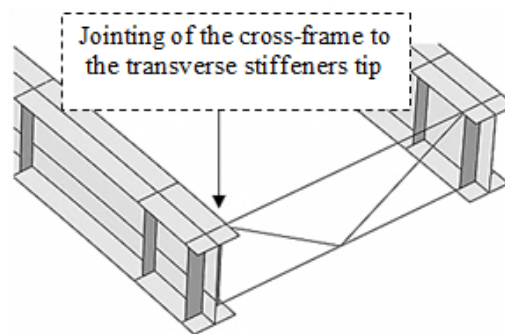


Fig. 2 Cross-frame modeling technique - Using beam elements

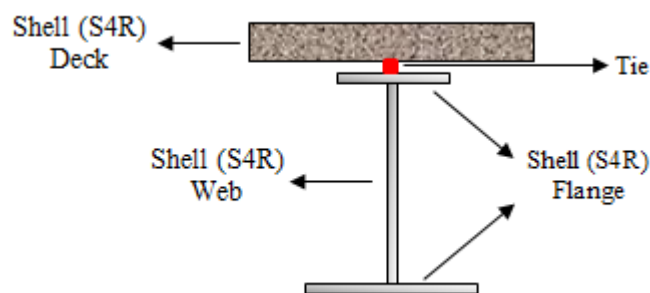


Fig. 3 Jointing of the concrete slab to compressive flange of the girder

## 4. VERIFICATION OF SIMULATION PROCESS

In order to evaluate the proposed simulating technique, the results obtained from numerical analysis for both composite and non-composite behavior of the curved bridge systems, were compared with previous numerical and experimental results. The numerical analyses were performed by the finite element software package of ABAQUS and both geometric and material nonlinearities have been considered. The analyses were done using General static and modified Riks method which has the ability to detect the full equilibrium path of the structure. Von Mises' yield criterion and the associated flow rule were used to define the plasticity of steel.

### 4.1. Verification of non-composite curved bridge behavior

In order to evaluate the non-composite behavior, the bending test sample B1 was selected from the seven samples tested by Hartmann (Hartmann 2005). As shown in

Fig. 4, B1 girder is located in the middle of G3 girder. S4R and B31 elements were used to model the girder components and the cross-frames, respectively. All the geometrical and material properties, distribution of residual stresses, and the support and loading conditions of the mentioned experiment are available in the cited reference. The material properties of the test sample B1 are shown in Fig. 5(a). Considering the geometrical and material nonlinearities, B1 girder was analyzed. In Fig. 5(b), the normalized B1 mid-span moment with respect to the strong-axis yield moment ( $M_x^{yield} = 5070 \text{ kN.m}$ ), is plotted versus the mid-span vertical displacement. As seen in this figure general trend of all the curves are the same. However, the maximum of experimental curve is lower. The reason of this is that the moment effect due to the weight of the bridge and test equipment in the experimental curve is not considered in reference (Hartmann 2005) and in fact, start point of the two diagrams are not equal. According to the test report, the total moment that can be resisted by sample B1 (including the sum of moments resulting from the self-weight effects and point loading) is equal to 4539.2 kN.m, which is very close to the maximum bending capacity predicted by the finite element simulation, with a maximum difference of 4%.

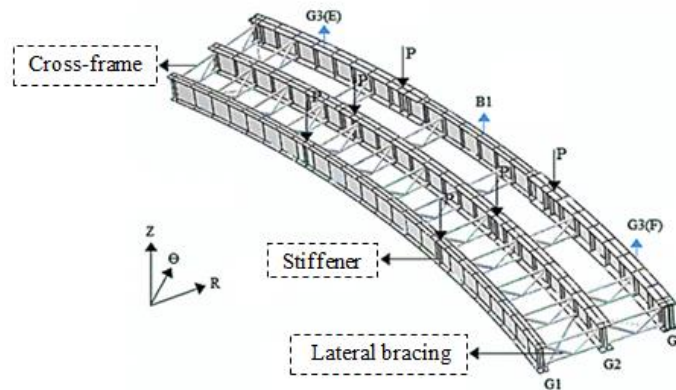
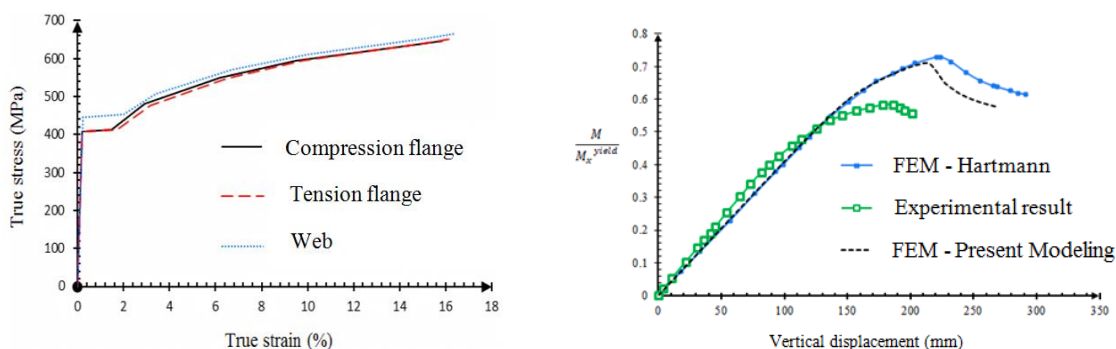


Fig. 4 ABAQUS model of Hartmann's test



a) B1 material properties

b) Comparing the B1 test mid-span moments and finite element predictions

Fig. 5 Material and Comparison of the test and FEM predictions

#### 4.2. Verification of composite curved bridge behavior

In order to evaluate the composite behavior simulation, the curved bridge of Jung's research (Jung 2006) was selected. In that research, the strength of the composite curved bridge system was studied experimentally and analytically under the design live load of AASHTO, as a part of CSBRP project. It must be noted that, the design live load of AASHTO contains two different loads: vehicular live load and linear load (AASHTO). The critical location of these loads is determined using the influence surface method. The geometrical and load properties of this experimental research have been described in the mentioned reference. Boundary conditions and general scheme of the curved bridge system are shown in Fig. 6. As seen in this figure, to investigate the deck uplift, two spring elements were used. These nonlinear springs were flexible in tension and rigid in compression.

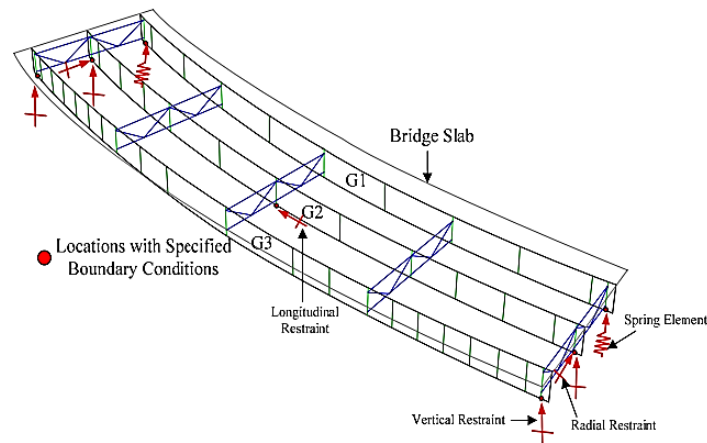
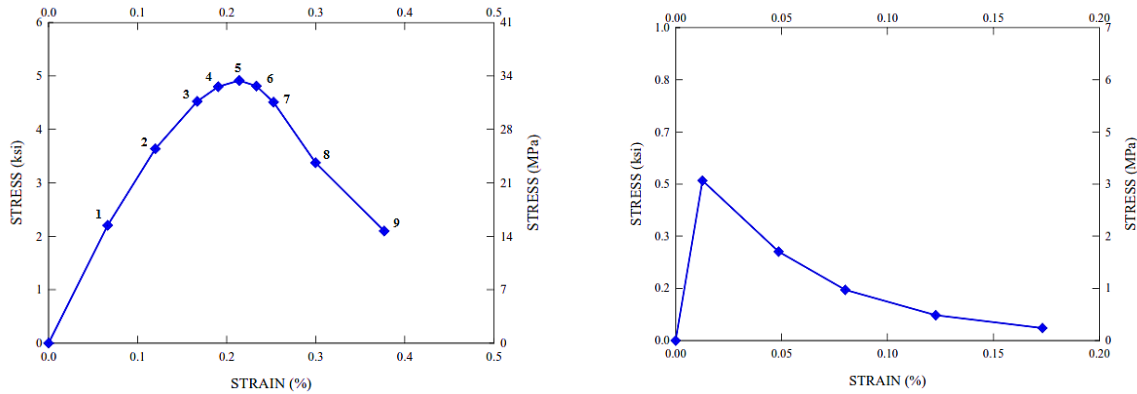


Fig. 6 Boundary condition of the finite element model (Jung 2006)

##### 4.2.1. Material properties

According to the reference (Jung 2006), the top and bottom flange of G1 girder and the top flange of G3 girder were made of grade 50 steel and the bottom flange of G3 girder is made of HPS70 steel. The stress-strain curves of the concrete, obtained based on the average of test data, are shown in Fig. 7. The average compressive strength of the concrete, as seen in Fig. 7(a), is equal to 33.58 MPa. The initial yield stress of compressive concrete based on ACI 318 definition is  $0.45f'_c$ , which is equal to 15.11 MPa. As well, the elastic modulus of concrete,  $E_c$ , is equal to the slope of the connected line of zero compressive stress to the stress of  $0.45f'_c$ . The average tensile strength of the concrete according to Fig. 7(b) is  $f_{ct}=3.45\text{MPa}$ .



a) Compressive stress-strain curve of the concrete      b) Tensile curve of the concrete (Jung 2006)

Fig. 7 Material and Comparison of the test and FEM predictions

#### 4.2.2. Numerical analysis results

The experimental and numerical curves of total applied load versus mid-span vertical displacement, and also versus reaction force of G1, G2, and G3 girders, are represented in Figs. 8-9, respectively. As seen in these figures, there is a good agreement between FEM results of this study and experimental results. For a further validation of the simulation method, the crack propagation pattern in the concrete slab at ultimate bearing moment was studied. Fig. 10 compares the experimental and numerical crack patterns of concrete slab, which corroborates the validity of the present modeling. It must be noted that, due to symmetry of the bridge, results have been shown only for half of the bridge. Comparing the tensile and compressive flange stresses with the numerical results of the reference (Jung 2006), shows that proposed methodology of concrete-steel interaction simulation is an appropriate method.

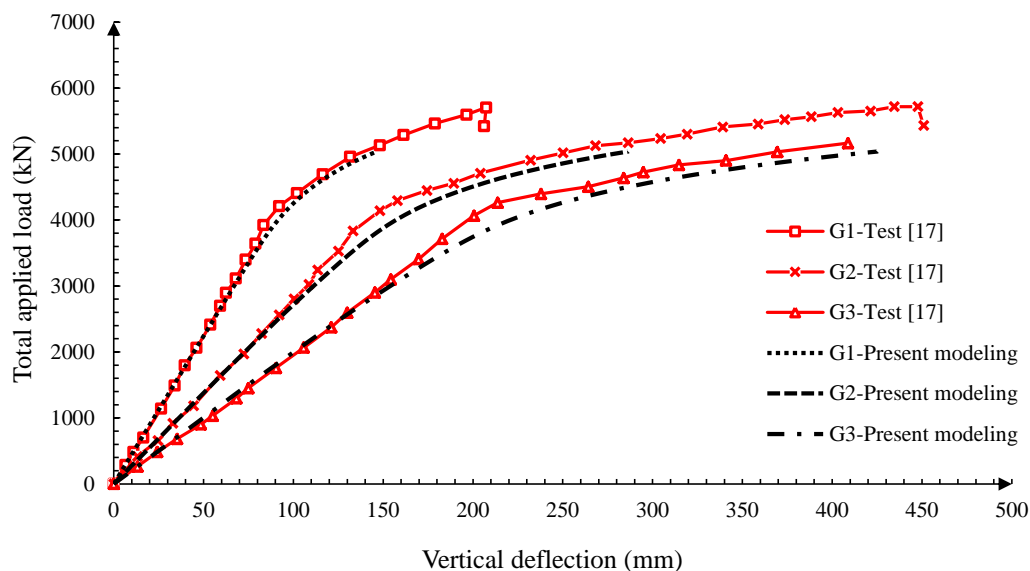


Fig. 8 Experimental and numerical curves of mid-span vertical displacement

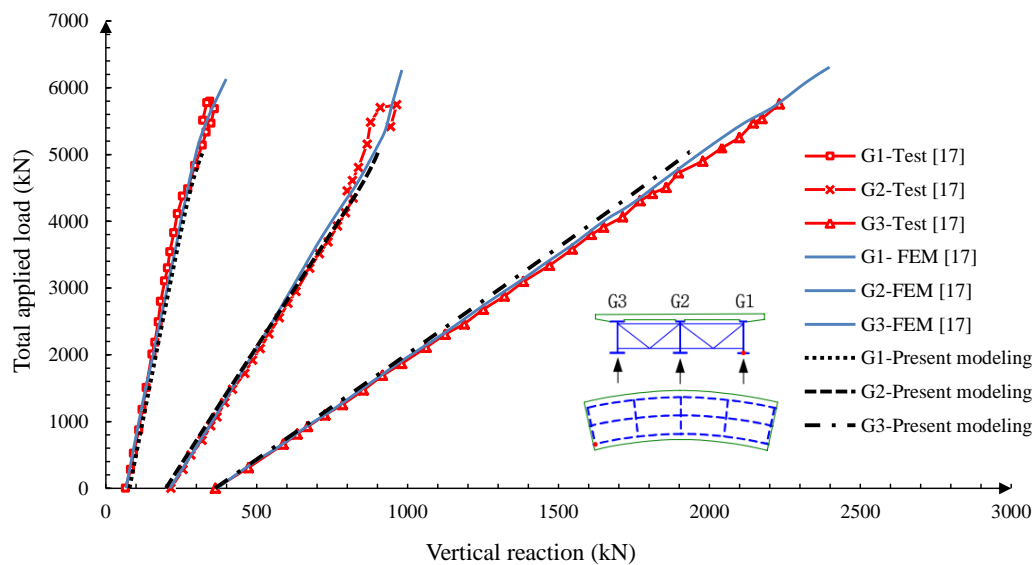
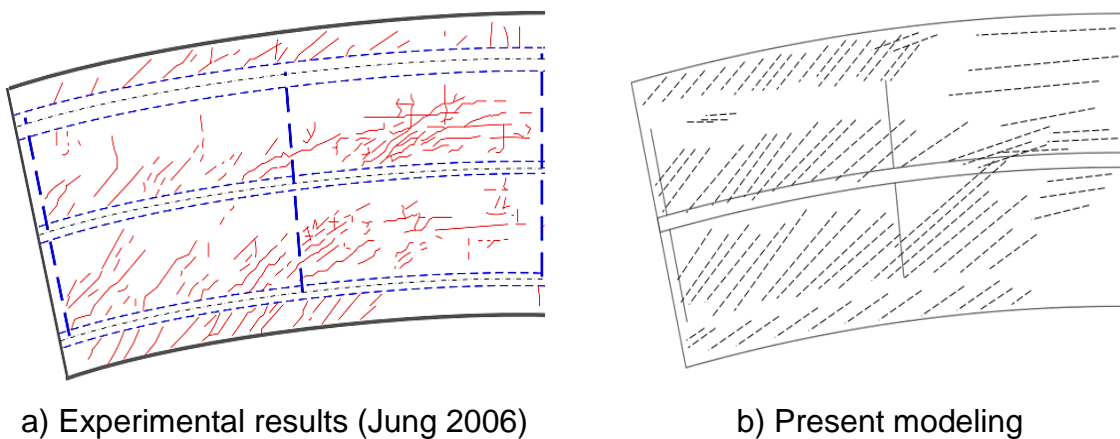


Fig. 9 Experimental and numerical curves of mid-span vertical reaction at supports



a) Experimental results (Jung 2006)                      b) Present modeling  
 Fig. 10 Observed and calculated crack pattern at the bottom face of concrete slab

## 5. CONCLUSIONS

Using ABAQUS software, an efficient method for simulating composite deck is presented. The main idea of present study are using S4R shell element to simulate both concrete slab and components of steel I-girders as well tie constraint to simulate composite action. It is shown that, this technique is superior to other prevalent methods, both for higher precision and less time needed to create the model. It is also shown that, if S4R shell element or C3D8R solid elements is used for simulating the concrete slab, along with tie constraint, the girder section stresses are accurately estimated. Calculated response curves of the deck, and calculated crack pattern of concrete slab were in a good agreement with the results of available experiments. However, according to modeling procedure, using solid element for slab, and Shell-to-Solid-Coupling constraint, leads to accurate load-displacement curve and tensile flange

stress values but the calculated compressive flange stresses are far from real stress distributions.

## 6. REFERENCES

- AASHTO (2012). *Bridge Design Specifications*, American Association of State Highway and Transportation Officials, Washington DC.
- Ashour, O. (2010). Effects of replacing cross frames with diaphragms on curved bridge construction, The Pennsylvania State University.
- Barr P.J., Eberhard M.O. and Stanton J.F. (2001), "Live-load distribution factors in prestressed concrete girder bridges." *Journal of Bridge Engineering*, **6**(5), 298-306.
- Barth, K.E. and H. Wu (2006), "Efficient nonlinear finite element modeling of slab on steel stringer bridges." *Finite Elements in Analysis and Design*, **42**(14), 1304-1313.
- Baskar K, Shanmugam N. and Thevendran V (2002), "Finite-element analysis of steel-concrete composite plate girder." *Journal of Structural Engineering*, **128**(9), 1158-1168.
- Biggs R.M., Barton F.W., Gomez J.P., Massarelli P.J. and McKeel Jr W.T. (2000), "Finite element modeling and analysis of reinforced-concrete bridge decks."
- Brockenbrough, R. L. (1986), "Distribution factors for curved I-girder bridges." *Journal of Structural Engineering*, **112**(10), 2200-2215.
- Chan, T. H. and J. H. Chan (1999), "The use of eccentric beam elements in the analysis of slab-on-girder bridges." *Structural Engineering and Mechanics*, **8**(1), 85-102.
- Chang, C.-J. and D. W. White (2008), "An assessment of modeling strategies for composite curved steel I-girder bridges." *Engineering Structures*, **30**(11), 2991-3002.
- Chen, Y. (1999). "Distribution of vehicular loads on bridge girders by the FEA using ADINA: modeling, simulation, and comparison." *Computers & structures*, **72**(1): 127-139.
- Chung, W. and E. D. Sotelino (2006), "Three-dimensional finite element modeling of composite girder bridges." *Engineering Structures*, **28**(1), 63-71.
- Cullen, L. E. (2007), *An Evaluation of the Strength Characteristics of Horizontally Curved Steel I-girder Bridges*, ProQuest.
- Davidson, J. S., et al. (1996), "Cross-frame spacing and parametric effects in horizontally curved I-girder bridges." *Journal of Structural Engineering*, **122**(9), 1089-1096.
- Hartmann, J. L. (2005), "An experimental investigation of the flexural resistance of horizontally curved steel I-girder systems."
- Hassel, H. L. (2011), "An analytical evaluation of distortion-induced fatigue in steel bridges."
- He J., Liu Y., Chen A. and Yoda T. (2010), "Experimental study on inelastic mechanical behaviour of composite girders under hogging moment." *Journal of Constructional Steel Research*, **66**(1), 37-52.
- Hibbitt H., Karlsson B. and Sorensen P. (2012), *ABAQUS Theory Manual, Version 6.12*. Pawtucket, Rhode Island, USA.
- Jung, S.-K. (2006), "Inelastic strength behavior of horizontally curved composite I-girder bridge structural systems."
- Lin J., Fafard M., Beaulieu D. and Massicotte B. (1991), "Nonlinear analysis of composite bridges by the finite element method." *Computers & structures*, **40**(5), 1151-1167.

- Mabsout M.E., Tarhini K.M., Frederick G.R. and Tayar C. (1997), "Finite-element analysis of steel girder highway bridges." *Journal of Bridge Engineering*, **2**(3), 83-87.
- Maneetes, H. (2001), "The effects of cross-frame geometry on the dynamic response of curved steel i-girder bridges during construction", Ph.D. Dissertation, The Pennsylvania State University.
- Ozgun, C. (2007). "Behavior and Analysis of a Horizontally Curved and Skewed I-girder Bridge."
- Sanchez, T. A. (2011), "Influence of bracing systems on the behavior of curved and skewed steel I-girder bridges during construction."
- Shahawy, M. and D. Huang (2001), "Analytical and field investigation of lateral load distribution in concrete slab-on-girder bridges." *ACI Structural Journal*, **98**(4).
- Shapiro, K. (2007), "Finite-Element Modeling of a Damaged Prestressed Concrete Bridge."
- Sharafbayani, M. and D. Linzell (2014). "Optimizing Horizontally Curved, Steel Bridge, Cross-Frame Arrangements to Enhance Construction Performance." *Journal of Bridge Engineering*, **19**(7).
- Si Larbi A., Ferrier E. and Hamelin P. (2009), "Concrete to steel lap joint failure criteria under combined shear and peeling stress." *Journal of Constructional Steel Research*, **65**(2), 386-394.
- Tabsh, S. W. and M. Tabatabai (2001). "Live load distribution in girder bridges subject to oversized trucks." *Journal of Bridge Engineering*, **6**(1), 9-16.
- Thevendran V., Chen S., Shanmugam N. and Richard Liew J. (1999). "Nonlinear analysis of steel-concrete composite beams curved in plan." *Finite Elements in Analysis and Design*, **32**(3), 125-139.